Materials Research. 2020; 23(1): e20190582
DOI: https://doi.org/10.1590/1980-5373-MR-2019-0582

Microstructural Evolution and Mechanical Properties of As-Cast Mg-12Zn Alloys with Different Al Additions

Yu Zhang[a,b]*, *Ming Li*[a,b], *Wen-Long Yang*[a,b], *Zong-Gang Wang*[a,b], *Xue-Zhi Wang*[a,b]

[a] *Hexi University, College of Physics and Electromechanical Engineering, Zhangye, China*
[b] *Hexi University, Institute of Advanced Material Forming Technology, Zhangye, China*

Received: October 22, 2019; Revised: January 09, 2020; Accepted: January 29, 2020.

In this study, Mg-12Zn magnesium alloys alloyed with Al additions (0, 2, 4, 6, 8 and 10, wt.%) were fabricated by permanent mould casting. The Al content on their microstructure and mechanical properties were systematically examined with an optical microscope (OM), a scanning electron microscope (SEM), an X-ray diffractometer (XRD) and mechanical tests at room temperature. The experimental results indicate that the microstructure of the alloys is mainly composed of α-Mg and semi-continuous or continuous eutectic phases. A higher addition of Al (≥6%) causes the generation of the $Mg_{17}Al_{12}$ phases. Notably, the grain sizes of the alloys gradually decrease, whilst the partial morphology of some eutectic phases is modified into lamellar structure with increasing of Al addition. Mechanical properties characterization manifested that, the alloys with different Al additions reveal distinguishing tensile properties. Among them, the alloy with 4% Al provides an excellent mechanical properties, i.e., a UTS of 206 MPa and an EL of 7.92%, which is respectively higher 28 MPa and 1.08% than that of ZA120 alloy. The deterioration in the tensile properties for the higher Al-bearing alloys is possibly related to the lamellar structure, coarse and continuous net-work morphology and β-$Mg_{17}Al_{12}$ phases, respectively.

Keywords: *Mg-12Zn magnesium alloy, Al addition, microstructure, mechanical property, β-$Mg_{17}Al_{12}$ phase.*

1. Introduction

Magnesium and its alloys are considered to be the lightest metallic structural materials at present. They have the advantages of low density, high specific strength and stiffness, good damping, shock absorption and mechanical processing performance, and have been widely used in rail transit, aerospace, electronic communication industry and other fields[1-3]. In recent years, the nations of the world attaches great importance to the research of magnesium and magnesium alloys, and has made plans for the research, development and application of magnesium alloys. Among them, there are many studies on Mg-Al-Zn (AZ) series and its multi-component magnesium alloys, such as AZ31, AM50A, AM60B and AZ91, were developed for industry applications. However, the existence of many β-$Mg_{17}Al_{12}$ phases in these alloys seriously affects the properties of the alloys mentioned. As a result, their widespread applications in engineering are severely restricted. The previously published findings manifest that, the brittle β-$Mg_{17}Al_{12}$ phase is prone to crack and the crack usually propagates along the interface between β-$Mg_{17}Al_{12}$ phase and Mg matrix, resulting in large cracks on the fracture surface[4]. Similar investigation has also been mentioned[5], α-Mg matrix has a HCP structure, while β-$Mg_{17}Al_{12}$ phase possesses a BCC structure, which causes the interface between α-Mg matrix and β-$Mg_{17}Al_{12}$ phase to become fragile, leading to the formation of micro-cracks at Mg/β-$Mg_{17}Al_{12}$ phase interface. It is worth mention that β-$Mg_{17}Al_{12}$ phase in Mg-Al system alloys will undergo softening and cannot play a role in hindering grain boundaries slide when the service temperature exceeds 393 K[6]. From that it can be concluded that, $Mg_{17}Al_{12}$ phase is not only sensitive to crack generation, but also a weakened phase in these alloys. Therefore, aiming at improving of microstructure and properties of the Mg-Al-Zn system alloys has become a critical issue at present. Fortunately, it is reported that Mg-Al alloy containing high content of Zn exhibits fine castability and mechanical properties at ambient[7].

As is known to all, Mg-Zn-Al (ZA) magnesium alloys with high Zn and low Al have been proposed as a low-cost, creep-resistant and diecastable alloy[8,9], which has a remarkable heat treatment strengthening characteristics. Meanwhile, the main precipitated phases of the alloys include $Mg_{32}(Al, Zn)_{49}$ and/or MgZn, which have a good strengthening effect. It is further reported[10] that the ZA series alloys show mechanical properties superior to that of the AZ series alloy in both room temperature and high temperature, and have a broad commercial application prospect comparable to that of the AZ system alloys. Currently, plentiful researches have been carried out on the design, microstructure and properties of the ZA series alloys at home and abroad. Abundant investigations on ZA series alloy seem to suggest that it is a promising candidate for developing high performance magnesium alloys. According to our previous study[11], the Zn/Al ratio has a significant influence on the formation of the phase in ZA series alloys, which affects the properties of the alloys. Wan[12] et al. investigated the microstructure, mechanical properties and creep resistance

*e-mail: zhangyu_lut@163.com

of Mg-(8%-12%)Zn-(2%-6%)Al alloys and pointed out that, the ZA82, ZA102 and ZA122 alloys are mainly composed of α-Mg, ε-$Mg_{51}Zn_{20}$ and τ-$Mg_{32}(Al,Zn)_{49}$ phase, the alloys ZA84, ZA104 and ZA124 contain α-Mg and τ phases, the ZA86, ZA106 and ZA126 alloys consist of α-Mg, τ precipitates, ϕ-$Al_2Mg_5Zn_2$ eutectics and β-$Mg_{17}Al_{12}$ compounds. Although the previously mentioned studies about ZA series alloys have been reported abundantly. But up to now, very little information pertaining to the microstructural evolution and mechanical properties of Mg-12Zn based alloys with the addition of Al has been reported so far. Furthermore, it is of great interest to explore the Zn/Al ratio possible cumulative effects on phase composition of ZA series alloys. Hence, based on the reports of ZA series alloys and previous studies, Mg-12Zn-*x*Al alloys (0, 2, 4, 6, 8 and 10, wt.%) alloyed with different additions of Al were designed and investigated systematically, so as to provide a reference for the research and development of new type ZA alloys.

2. Experimental procedure

The investigated alloys were prepared from commercial high purity Mg (>99.99%), Zn (>99.999%), Al (>99.99%) ingots. Six sample alloys with the nominal compositions were shown in Table 1 and noted ZA120, ZA122, ZA124, ZA126, ZA128 and ZA1210 (all compositions are in wt.% hereinafter), respectively. The smelting plays a significant role in the alloy fabrication, to ensure the purity of the studied alloys, the Mg, Zn and Al ingots were polished off by a steel brush before preheating. The weight of 2.0 kg of each alloy was melted in a mild steel crucible placed in an electric resistance furnace under a high-purity argon atmosphere and a covering agent RJ-2 protection. After the Mg ingot was completely melted, the Zn and Al ingots were added into the melt at 680 °C. When the liquid melt temperature was slowly rised to approximately 750 °C, and then was held at 750 °C for 20 min to guarantee the homogeneity of alloying elements. Subsequently, the melt was manual stirred by using 2% (ratio to the whole raw metal) C_2Cl_6 at 730 °C. After thorough refining, the liquid melt was isothermally maintained for 20 min at 710 °C for the settlement of inclusions. Then, the liquid melt was poured into the metallic mold which was coated and preheated to a temperature of about 200 °C with dimensions of length (210 mm), height (130 mm) and breadth (85 mm).

Table 1. Chemical compositions of the investigated alloys

Alloy code	Nominal compositions (wt.%)
ZA120	Mg-12Zn
ZA122	Mg-12Zn-2Al
ZA124	Mg-12Zn-4Al
ZA126	Mg-12Zn-6Al
ZA128	Mg-12Zn-8Al
ZA1210	Mg-12Zn-10Al

For the best results, the specimens for OM and SEM observation were mechanically polished with grinding and polishing papers, and then etched by a 4 vol % HNO_3 solution at room temperature. The microstructures of the specimens were subsequently observed by an optical microscope (OM, MeF-3) and a scanning electron microscopy (SEM, 450) equipped with an energy dispersive spectroscope (EDS). The phase compositions in the experimental alloys were analyzed by a D/max-2400 X-ray diffraction (XRD) at 40 kV and 40 mA using Cu Kα radiation with a scanning velocity of 5 °/min and a step scanning 2θ from 10° to 90°. The tensile specimens with a gauge section of 15 mm × 2 mm × 3 mm were machined from the bottom of obtained ingots by using a computer numerical-controlled wire-cutting machine, as shown in Figure 1. The mechanical tests were carried out by WDW-100D type electromechanical universal testing machine with a loading rate of 1 mm/s at room temperature. Three specimens were tested for each alloy and the average values were presented as the results of ultimate tensile strength (UTS) and elongation to failure (EL). The transverse fracture surfaces of the tensile specimens were also examined by SEM.

3. Results and discussion

3.1 As-cast microstructure

The XRD profiles of the Mg-12Zn alloys containing different additions of Al are presented in Figure 2. It can be seen from Figure 2a that both α-Mg phase and $MgZn_2$ phase exist in ZA120 alloy. In contrast, the new diffraction peaks of Mg_2Zn_3 and $Mg_{32}(Al,Zn)_{49}$ phase are observed for the Al-containing alloys. The ZA122 and ZA124 alloys consist of four phases, i.e., α-Mg, Mg_2Zn_3, $Mg_{32}(Al,Zn)_{49}$ and Mg_7Zn_3 phases. According to the previous investigation[13], the Mg_7Zn_3 binary phase will generate in Mg-Zn-Al alloy when the mass ratio of Zn/Al is more than 2. As for mentioned MgZnAl intermetallic compound, it has a body-centered cubic structure (space group $Im\bar{3}$, a=1.416 nm[14]), meanwhile possesses a high melting point and good thermal stability. With Al addition further increasing, as observed from Figure 2 that, additional diffraction peaks of $Mg_{17}Al_{12}$ phase emerge

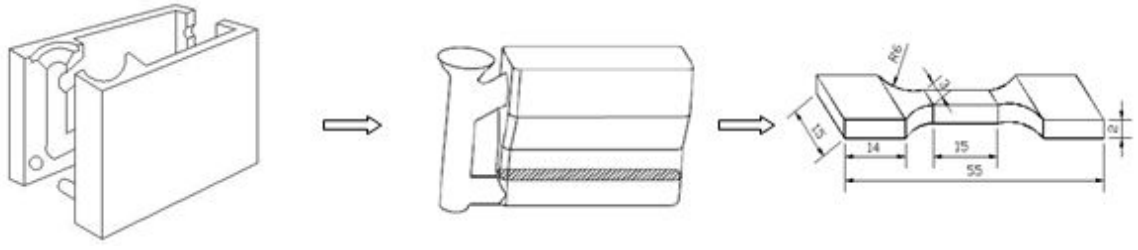

Figure 1 - Schematic for permanent mold, ingot and dimension of tensile sample (unit: mm).

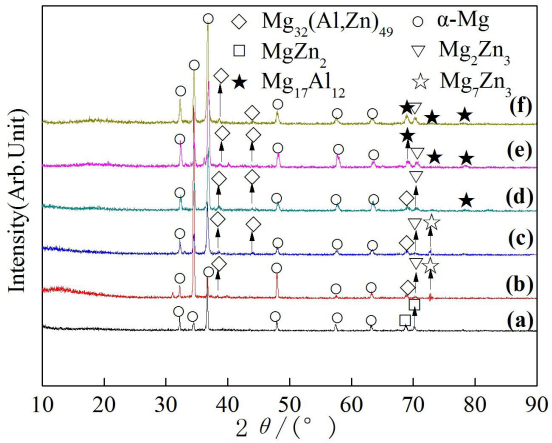

Figure 2 - XRD patterns of the as-cast alloys: (a) ZA120 alloy; (b) ZA122 alloy; (c) ZA124 alloy; (d) ZA126 alloy; (e) ZA128 alloy; (f) ZA1210 alloy.

in ZA126, ZA128 and ZA1210 alloys,and peaks emerge corresponding to the $Mg_{17}Al_{12}$ phase tends to increase with increasing of Al addition. It is confirmed that $Mg_{17}Al_{12}$ phase has a body-centered cubic structure with a lattice parameter a=1.06 nm[15]. Despite the above analysis, the reason for the formation of the intermetallic compounds in the Al-bearing alloys is not completely clear and further study is needed. Through the above analysis, it can be summarized that the Zn/Al mass ratio has a significant influence on the phase composition of the investigated alloys. Namely, if the mass ration of Zn/Al is less than 2, the Mg_2Zn_3, $Mg_{32}(Al,Zn)_{49}$ and $Mg_{17}Al_{12}$ intermetallic compounds exist in the as-cast microstructure alloy. The reason is that the addition of excessive Al makes the Al atom at the front of solid-liquid interface combine with Zn atom under non-equilibrium solidification conditions, leading to the generation of form $Mg_{17}Al_{12}$ phases. On the contrary, when the Zn/Al mass ratio more than 2, Mg_2Zn_3, $Mg_{32}(Al,Zn)_{49}$ and Mg_7Zn_3 phases are be detected in the as-cast microstructure alloy. The eutectic compounds of the investigate alloy with Zn/Al mass ratio 2 consist of Mg_2Zn_3, $Mg_{32}(Al,Zn)_{49}$ and $Mg_{17}Al_{12}$.

The OM and SEM micrograph images of as-cast Mg-12Zn alloys with different Al additions are demonstrated in Figure 3, where it can be found that the alloys have a typical dendrite configuration with interphases at interdendritic regions, the volume fraction of which increases with increasing of Al addition in the Al-containing alloys. The resultant microstructures of the alloy are mainly composed of primary α-Mg, non-equilibrium eutectic phase with continuous or semi-continuous precipitated along grain boundaries and tiny irregular granular phases in the interior of the grain. The morphology of eutectic phases of the alloys is gradually evolved from an isolated island into a coarse and continuous netlike, the size and the number of the secondary phases gradually increases, whereas the size of the grains gradually decreases with an increment of Al addition.

It is well known that the size and morphology of dendrite grains are mainly determined by heterogeneous nucleation and solute segregation[16]. As shown in Figure 3a and b, the microstructures of the ZA120 alloy are mainly comprised of coarse α-Mg grains and intermetallic compounds with an isolated island and granular form. When the 2% Al is added to Mg-12Zn alloy, the corresponding microstructural analysis shown in Figure 3c and d. It indicates that the microstructures of the alloy reveal still developed dendritic morphology. Moreover, the eutectic phases in ZA122 alloy are aggregated in some regions, the isolated particles and grain sizes tend to decrease, as compared to the ZA120 alloy. With 4% Al addition, it is observed from Figure 3e and f that the grain size of the ZA124 alloy is dramatically smaller than that of the ZA120 alloy, the morphology of eutectic phase distributed along grain boundary tends to be fine, and the number of eutectic phase is more than that of ZA120 alloy. According to the XRD patterns, the increased phases should be Mg_2Zn_3, $Mg_{32}(Al,Zn)_{49}$ and Mg_7Zn_3. In contrast, with 6% Al addition, as illustrated in Figure 3g and h, it is distinct that most of the eutectic phases exist as networks along the grain boundaries, while some particles are dispersed inside the grains. Interestingly, it is necessary to note that the distribution of the secondary phases has prominent dendrite segregation (marked by blue elliptic region), and the number of secondary phases increases obviously. Additionally, one can see that the grain size of the alloy further decreases. When the 8% Al is added to Mg-12Zn alloy, it can be found from Figure 3i and j that the morphology of eutectic phases appears to be similar to that of the ZA126 alloy. Apparently, the grains size decreases considerably while the number of eutectic phases of the ZA128 alloy increases significantly (comparing Figure 3a, c, e, g). Meanwhile, the presentation of dendrite segreation tends to be more obvious, and grain boundaries seem to be demonstration conspicuous trend of broadening. When the addition of Al is further increased to 10%, as shown in Figure 3k and l, where further grain refinement effect and the highest value of the volume fraction of the secondary phase can be obtained with the Al addition higher than 8% in the alloy, meanwhile the grain size of the alloy is the smallest among those of the studied alloys. This is mainly due to a higher addition of Al results in the Al enrichment during the solidification, then induces constitutional undercooling in a diffusion layer ahead of the solid/liquid interface and suppresses grain growth thus leading to the grain refinement. Similarly, the primary grains with different morphologies can still be found. Furthermore, the distribution of the secondary phases penetrates the interdendritic regions and demonstrates coarsely and continuously network. Simultaneously, the evident dendrite segregation (marked by blue elliptic region) still can be observed in the ZA1210 alloy.

It should be emphasized that the phase structure and its component depend mainly on the composition of the alloy. Figure 4 displays the high magnification SEM micorgraph images of the investigated alloys, where the elementary composition of the typical ZA120, ZA124 and ZA1210 alloys was point-analyzed by EDS and the EDS results are presented in Table 2. By comparison, it can be seen from Figure 4, after being modified by adding diffenent Al, the morphology of the secondary phases is altered predominantly. Evidently, the local regions of eutectis compounds of the Al-bearing alloys reveal obvious lamellar structure, whose volum fraction

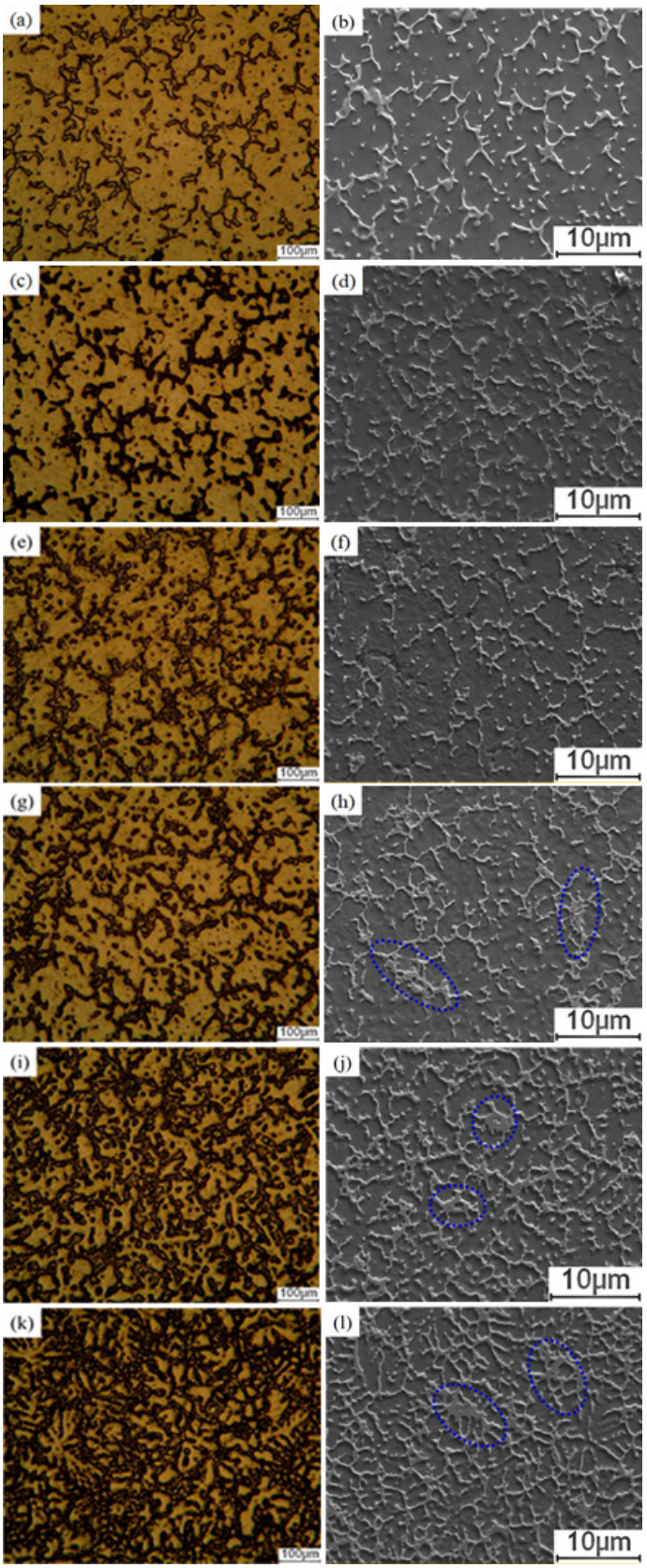

Figure 3 - Optical (a, c, e, g, i, k) and SEM (b, d, f, h, j, l) micrographs of the as-cast alloys: (a, b) ZA120 alloy; (c, d) ZA122 alloy; (e, f) ZA124 alloy; (g, h) ZA126 alloy; (i, j) ZA128 alloy; (k, l) ZA1210 alloy.

Table 2. EDS results of the as-cast alloys (at.%)

Location (point)	Mg	Zn	Al
Figure 4(a), A	80.40	19.60	0.00
Figure 4(a), B	78.91	21.09	0.00
Figure 4(c), A	75.62	19.38	5.00
Figure 4(c), B	72.74	25.36	1.90
Figure 4(c), C	71.04	20.98	7.98
Figure 4(f), A	63.12	18.05	18.83
Figure 4(f), B	63.17	18.34	18.49
Figure 4(f), C	67.63	22.27	10.10

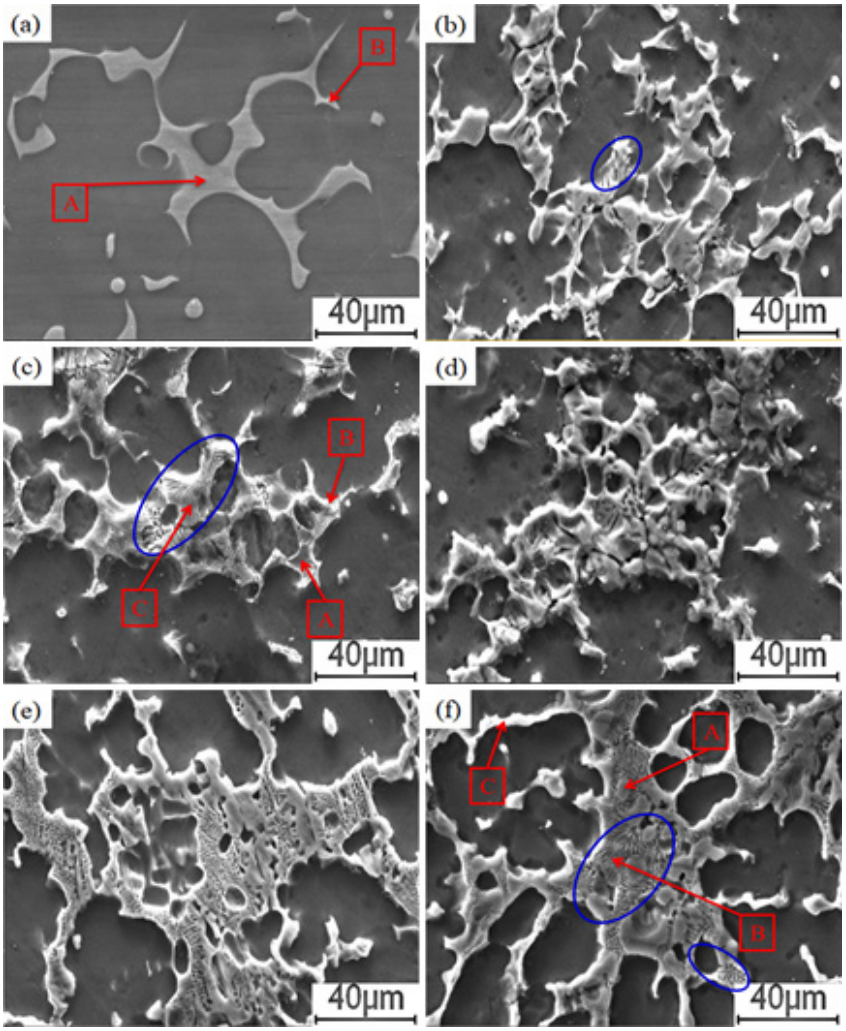

Figure 4 - SEM high-magnification micrographs of the as-cast alloys: (a) ZA120 alloy; (b) ZA122 alloy; (c) ZA124 alloy; (d) ZA126; (e) ZA128; (f) ZA1210.

tends to be increasement with increasing of Al addition. Furthermore, the partial gray or black precipitates along the grain boundary were replaced by bright precipitates unevenly dispersed in the edge of the whole eutectic phases.

For the ZA120 alloy without Al, as shown in Figure 4a, the eutectic compound presents a smooth island morphology, which is composed of bright phase and gray one. On the basis of XRD results (Figure 2a) and EDS analysis, the gray precipiate (marked by A) can be confirmed as α-Mg and $MgZn_2$ phase. The bright precipitate (marked B) is rich in Zn. Combined with the XRD results, the bright one is identified as $MgZn_2$ phase. With 2% Al addition, it is seen from Figure 4b that the partial eutectic phases of the alloy show lamellar morphology (marked by elliptical circle). Obviously, there are existing three main phases in the eutectic compound: the black, grey and bright phases,

respectively. After adding 4% Al, it also observed that from Figure 4c, similar eutectic morphology that of the ZA122 is also exhibited in ZA124 alloy. As seen in Table 2, the black precipitate (marked A) and gray one (marked C) includes Mg, Zn and Al, combining with the XRD results (Figure 2c), they are regarded as α-Mg and $Mg_{32}(Al,Zn)_{49}$. The composition of the bright precipitate (marked B) includes Mg, Zn and Al, and the content of Zn is distinctly higher than that in the other positions (marked A and C). It is found, from XRD result (Figure 2c) and EDS point analysis, that they are most likely comprised of the Mg_2Zn_3 and Mg_7Zn_3 phases. After 6% and 8% Al is added, as shown in Figure 4d and e, almost half of the eutectic phases show lamellar morphology. Furthermore, the eutectic morphology has a tendency to become coarser. When the Al addition increased to 10%, as shown in Figure 4f, for the ZA1210 alloy, the eutectic compounds appear mainly in the lamellar morphology. Meanwhile, the distribution of the partial secondary phases has modality characteristics of own, namely, some granular phases are embedded on the surface of the whole eutectic phase. The EDS results reveal that, the gray granular precipitate (marked A) contains Mg, Zn and Al, and the content of Al is higher than that the other ones (marked B and C). Therefore, according to the results of XRD (Figure 2f), it can be validated as $Mg_{32}(Al,Zn)_{49}$ phase. With the composition of black precipitate (marked B) corresponds to α-Mg and $Mg_{17}Al_{12}$ phase. Besides, the bright one (marked C) mainly includes Mg, Zn and Al, the content of Zn is higher than that the other ones (marked A and B). Hence, according to the results of XRD (Figure 2f) and EDS, it is inferred as Mg_2Zn_3 phase.

3.2 As-cast mechanical properties

Figure 5 displays the variations trend of the room temperature tensile properties when the Al additions varies from 0 to 10%, including the ultimate tensile strength (UTS) and elongation to failure (EL), respectively. As shown in Figure 5, the UTS and EL values firstly achieve an evident improvement with increasing Al addition and obtain maximum value when Al addition increase to 4%. And then they manifest the gradual reductions with more Al addition. It can be seen from Figure 5 that the UTS and EL of the Al-free alloy is 178 MPa and 6.84%, respectively. Distinctly, the alloys with the additions of 2% and 4% reveal relatively higher tensile properties than the binary alloy. This indicating that the addition of 2 ~ 4% Al to the binary alloy is conducive to the tensile properties of the alloys. It is worth mentioning that, the maximum values of UTS (206 MPa) and EL (7.92%) are simultaneously obtained from the 4% Al-containing alloy. Compared with the 2% Al alloy, the UTS and EL of the alloy are increased by 13 MPa and 6.59%, respectively. It is well known that the presence of fine and uniform phases distributed along grain boundaries is easier to act as an effective straddle to the dislocation motion thus improving the properties[17]. It can, thereby, be inferred that the increasement of tensile properties is mainly attributed to the grain refinement strengthening and secondary phase strengthening effects. Also, the fine and homogeneous distributed eutectic phases in the alloy act as obstacles to the movement of dislocations during the deformation process. Nevertheless, it is clearly found that from Figure 5, the addition of Al which is got up to 6% does not maintains continuous increase in UTS and EL except a apparent decrease (from 206 MPa to 171 MPa and from 7.92% to 5.78%), respectively. Indicating that fine grain strengthening does not play a leading role in improving mechanical properties, especially in ZA1210 alloy. It is well accepted that the mechanical properties of the alloy have an important relationship with the distribution, morphology, size and category of eutectic phase[18]. It is believed that the decrease of tensile properties of the Al-containing alloys can be explained by the following three aspects: (1) When the addition of Al exceeds 4%, with increasing of Al addition, the grains of the investigated alloys are gradually refined, but the primary α-Mg grains are almost surrounded by the coarsely and continuously interdendritic eutectic compounds, which can induce generation of the cracks and stress concentration at the interface between intermediate phase and matrix during deformation, thus leading to the deterioration of the tensile properties. (2) A higher addition of Al (≥6%) causes the generation of the $Mg_{17}Al_{12}$ intermetallics. Duley[19] pointed out that brittle particles often act as stress raisers and thereby, as crack initiation sites during deformation, resulting in inferior mechanical properties. Similar literature has been reported[20] that coarse β-$Mg_{17}Al_{12}$ phase is commonly considered to be detrimental to the plastic deformation of magnesium alloys. Furthermore, Nie[4] found out that brittle $Mg_{17}Al_{12}$ phase cracks easily and the cracks usually propagate along the interface of $Mg_{17}Al_{12}$ phase and Mg matrix. The above outcome means that the $Mg_{17}Al_{12}$ compounds play an adverse role in the incrseing of tensile properties of the studied alloys. It is

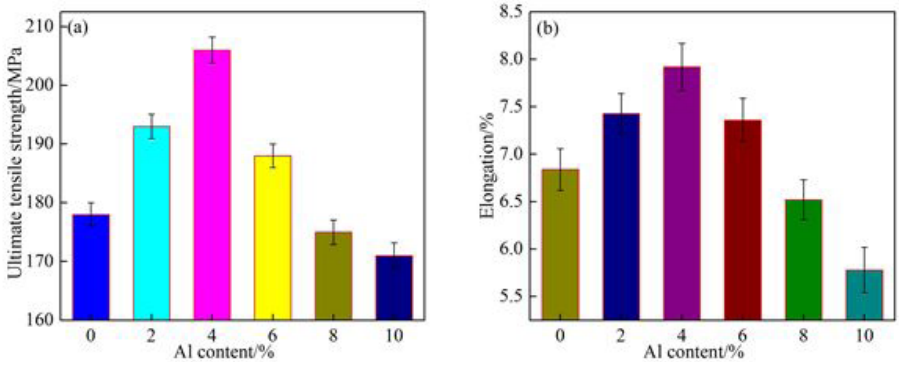

Figure 5 - Mechanical properties of the as-cast Mg-12Zn alloys with different Al content (a) tensile strength and (b) elongation.

reported that the lamellar eutectic microstructures possibly act as crack initiation sites during tensile test, thus leading to the relatively poor tensile properties[21]. (3) When the Al addition exceeds 4%, the local morphology of the eutectic phase is evolved into lamellar shape, which is possibly related to the deterioration of the mechanical properties. However, this needs to be further investigated.

By combining above the analysis, it can be summarized that the moderate addition of Al (2 ~ 4%) has an advantageous effect on the tensile properties of the investigated alloys at room temperature. More important, a higher addition of Al (≥6%) causes the grain refinement does not play a dominant role in improving mechanical properties.

The SEM images of tensile fracture surfaces of the studied alloys with different Al additions are shown in Figure 6. It is well accepted that the cleavage fracture, quasi-cleavage fracture and inter-granular fracture are the main fracture modes of magnesium alloys[22]. As shown in Figure 6, a number of

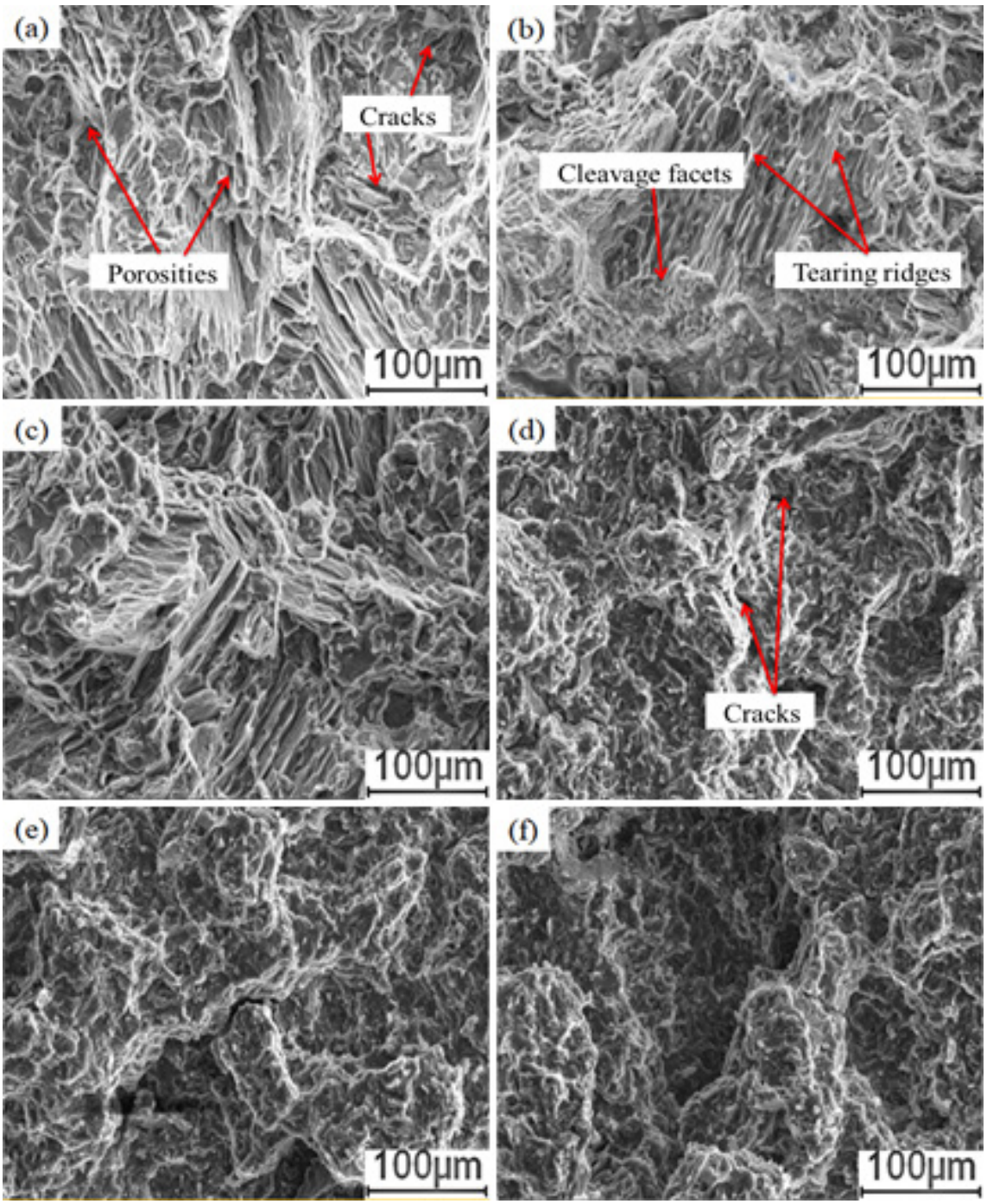

Figure 6 - SEM fractographs acquired from the investigated alloys (a) ZA120 alloy; (b) ZA122 alloy; (c) ZA124 alloy; (d) ZA126; (e) ZA128; (f) ZA1210.

cleavage facets with cleavage steps of various sizes, tearing ridges, a few porosities and micro-cracks can be clearly seen, respectively. Furthermore, some river patterns at some places are observed as well, indicating that all the tensile fracture surfaces have mixed fracture characteristics of cleavage and quasi-cleavage fractures. As shown in Figure 6a, some cleavage facets, tearing ridges, visible cracks and a few porosities are observed in the Al-free alloy. The generation of the porosity is ascribed to the developed primary dendrites. According to the report[23], the porosities induce the origination of cracks, and then the cracks grow and propagate along the dendrite boundaries to the final failure. As shown in Figure 6b, c, the fracture surfaces of the ZA122 and ZA124 alloys too reveale cleavage facets, tearing ridges and a few porosities. This manifesting that the additions of 2 ~ 4% to the binary alloy do not dramatically modify the fracture regime of the alloys. However, the area of the cleavage facets on the fracture surface of the ZA124 alloy tend to increases compared to that of the ZA122 alloy (seening Fig, 6b and c). In short, the ZA120, ZA122 and ZA124 alloys show typical quasi-cleavage fracture and cleavage fracture mode. A higher content Al (≥6%) addition the Mg-12Zn alloy does significantly change the fracture regime of the alloys. As observed in Figure 6d, e and f, the number of cleavage facets and tearing ridges decreases considerably, which are replaced by micro-cracks and numerous fractured secondary phases. This indicated that the fracture regime transformed to brittle fracture. On the basis of existing literature[24], the $Mg_{17}Al_{12}$ phases may facilitate the generation of micro-cracks and severe cracking of the particles at the grain boundary due to the their incompatibility with the α-Mg matrix.

4. Conclusion

(1) The ZA120 alloy mainly consists of α-Mg and $MgZn_2$ phase. Al addition results in not only the formation of Mg_7Zn_3 and Mg_2Zn_3 phase, but also the production of $Mg_{32}(Al,Zn)_{49}$ phase within the range of 2 ~ 4% Al. In addition, a higher addition of Al (≥6%) causes the generation of the $Mg_{17}Al_{12}$ compound.

(2) The addition of Al has a prominent effect on the morphology of eutectic phases of the investigated alloys. Namely, after adding Al to the ZA120 alloy, leading to the partial morphology of some eutectic phases is evolved into lamellar structure, and this evolution trend becomes more and more eident with incrseing of Al addition. Furthermore, the lamellar structure play a detrimental role in the tensile properties.

(3) The Zn/Al mass ratio has a significant influence on the mechanical properties of the investigated alloys. When the Zn/Al mass ratio more than 2,the addition of Al can enhances the mechanical properties, while the Zn/Al mass ratio less than 2, it deteriorates the mechanical properties. The alloy with Zn/Al ratio 2 exhibits excellent mechanical properties, i.e., a UTS of 206 MPa and an EL of 7.92%, which is respectively higher 28 MPa and 1.08% than that of the free-Al alloy. Therefore, the amount of Al addition to the binary alloy must be limited within a rational range.

(4) The microstructural parameters of these alloys, such as grains size, eutectic morphology, secondary phase distribution, and intermetallic compounds, demonstrate conspicuously different from each other. It is considered that the distribution, morphology, composition of eutectic phases, are a omnibus factor that affects the tensile properties of the investigated alloys.

5. Acknowledgements

The authors wish to express thanks to financial support from the Hexi University Headmaster Foundations of China (XZ2018014) and Hexi University doctor research initiation fundations of China.

6. References

1. Yuan GY, You GQ, Bai SL, Guo W. Effects of heat treatment on the thermal properties of AZ91D magnesium alloys in different casting processes. J Alloys Compd. 2018;766:410-6. http://dx.doi.org/10.1016/j.jallcom.2018.06.370.
2. Feng J, Sun HF, Li XW, Zhang J, Fang W, Fang WB. Microstructures and mechanical properties of the ultrafine-grained Mg-3Al-Zn alloys fabricated by powder metallurgy. Adv Powder Technol. 2016;27(2):550-6. http://dx.doi.org/10.1016/j.apt.2016.02.008.
3. Qi FG, Zhang DF, Zhang XH, Xu XX. Effect of Sn addition on the microstructure and mechanical properties of Mg-6Zn-1Mn (wt.%) alloy. J Alloys Compd. 2014;585:656-66. http://dx.doi.org/10.1016/j.jallcom.2013.09.156.
4. Nie KB, Wang XJ, Wu K, Hu XS, Zheng MY. Development of SiCp/AZ91 magnesium matrix nanocomposites using ultrasonic vibration. Mater Sci Eng A. 2012;540(4):123-9. http://dx.doi.org/10.1016/j.msea.2012.01.112.
5. Wang F, Ma DZ, Wang Z, Zheng L. Microstructure, mechanical properties and solidification behavior of AM50-*x*(Zn,Y) magnesium alloy. Chin Shu Hsueh Pao. 2016;52(9):1115-22. http://dx.doi.org/10.3724/SP.J.1037.2010.00146.
6. Tardif S, Tremblay R, Dube D. Influence of cerium on the microstructure and mechanical properties of ZA104 and ZA104+0.3Ca magnesium alloys. Mater Sci Eng. 2010;527(29-30):7519-29. http://dx.doi.org/10.1016/j.msea.2010.08.082.
7. Zhang Z, Couture A, Luo A. An investigation of the properties of Mg-Zn-Al alloys. Scr Mater. 1998;39(1):45-53. http://dx.doi.org/10.1016/S1359-6462(98)00122-5.
8. Xiao WL, Shen YS, Wang LD, Wu YM, Cao ZY, Jia SS, et al. The influences of rare earth content on the microstructure and mechanical properties of Mg-7Zn-5Al alloy. Mater Des. 2010;31(7):3542-9. http://dx.doi.org/10.1016/j.matdes.2010.01.046.
9. Wang F, Hu T, Zhang Y, Xiao W, Ma C. Effects of Al and Zn contents on the microstructure and mechanical properties of Mg-Al-Zn-Ca magnesium alloys. Mater Sci Eng A. 2017;704:57-65. http://dx.doi.org/10.1016/j.msea.2017.07.060.
10. Zhang J, Zuo RL, Chen YX, Pan FS, Luo XD. Microstructure evolution during homogenization of a t-type Mg-Zn-Al alloy. J Alloys Compd. 2008;448(1-2):316-20. http://dx.doi.org/10.1016/j.jallcom.2006.10.135.
11. Zhang Y, Huang XF, Ma ZD, Li Y, Guo F, Yang JC, et al. The influences of Al content on the microstructure and mechanical properties of as-cast Mg-6Zn magnesium alloys. Mater Sci Eng A. 2017;686:93-101. http://dx.doi.org/10.1016/j.msea.2016.12.122.
12. Wan XF, Ni HJ, Huang MY, Zhang HL, Sun JH. Microstructure, mechanical properties and creep resistance of Mg-(8%-12%) Zn-(2%-6%)Al alloys. Trans Nonferrous Met Soc China.

2013;23(4):896-903. http://dx.doi.org/10.1016/S1003-6326(13)62545-5.
13. Guan SK, Zhang CX, Wang LG, Wu LH, Chen PL, Tang YL. Phase selection of ternary intermetallic compounds during solidification of high zinc magnesium alloy. Transaction of Nonferrous Metals Society of China. 2008; 18 (3): 593-597.
14. Bourgeois L, Muddle BC, Nie JF. The crystal structure of the equilibrium Φ phase in Mg-Zn-Al casting alloys. Acta Mater. 2001;49(14):2701-11. http://dx.doi.org/10.1016/S1359-6454(01)00162-8.
15. Liu CQ, Chen HW, He C, Zhang YY, Nie JF. Effects of Zn additions on the microstructure and hardness of Mg-9Al-6Sn alloy. Mater Charact. 2016;113:214-21. http://dx.doi.org/10.1016/j.matchar.2016.01.021.
16. Kim YM, Wang L, You BS. Grain refinement of Mg-Al cast alloy by the addition of manganese carbonate. J Alloys Compd. 2010;490(1-2):695-9. http://dx.doi.org/10.1016/j.jallcom.2009.10.141.
17. Balasubramani N, Pillai UTS, Pai BC. Optimization of heat treatment parameters in ZA84 magnesium alloy. J Alloys Compd. 2008;457(1-2):118-23. http://dx.doi.org/10.1016/j.jallcom.2007.02.147.
18. Chen TJ, Zhang DH, Wang W, Ma Y, Hao Y. Effects of Y content on microstructures and mechanical properties of as-cast Mg-Zn-Nd alloys. China Foundry. 2015;12(5):339-48.
19. Duley P, Sanyal S, Bandyopadhyay TK, Mandal S. Homogenization-induced age-hardening behavior and room temperature mechanical properties of Mg-4Zn-0.5Ca-0.16Mn (wt%) alloy. Mater Des. 2019;164:107554-70. http://dx.doi.org/10.1016/j.matdes.2018.107554.
20. Niu YX, Song ZT, Le QC, Hou J, Ning FK. Excellent mechanical properties obtained by low temperature extrusion based on Mg-2Zn-1Al alloy. J Alloys Compd. 2019;801:415-27. http://dx.doi.org/10.1016/j.jallcom.2019.05.297.
21. Zhang Y, Huang XF, Li Y, Ma ZD, Ma Y, Hao Y. Effects of samarium addition on as-cast microstructure, grain refinement and mechanical properties of Mg-6Zn-0.4Zr magnesium alloy. J Rare Earths. 2017;35(5):494-502. http://dx.doi.org/10.1016/S1002-0721(17)60939-6.
22. Acer E, Çadırlı E, Erol H, Kırındı T, Gündüz M. Effect of heat treatment on the microstructures and mechanical properties of Al-5.5Zn-2.5Mg alloy. Mater Sci Eng A. 2016;662:144-56. http://dx.doi.org/10.1016/j.msea.2016.03.073.
23. Zhu SZ, Luo TJ, Li YJ, Yang YS. Characterization the role of squeezing pressure on microstructure, tensile properties and failure mode of a new Mg-6Zn-4Al-0.5Cu magnesium alloy. J Alloys Compd. 2017;718:188-96. http://dx.doi.org/10.1016/j.jallcom.2017.05.115.
24. Zhang WQ, Xiao WL, Wang F, Ma CL. Development of heat resistant Mg-Zn-Al-based magnesium alloys by addition of La and Ca: microstructure and tensile properties. J Alloys Compd. 2016;684:8-14. http://dx.doi.org/10.1016/j.jallcom.2016.05.137.